

Discovery and Characterization of Small Molecule Inhibitors of the BET Family Bromodomains

Chun-wa Chung,^{*,†} Hervé Coste,[§] Julia H. White,[†] Olivier Mirguet,[§] Jonathan Wilde,[†] Romain L. Gosmini,[§] Chris Delves,[†] Sylvie M. Magny,[§] Robert Woodward,[†] Stephen A. Hughes,[†] Eric V. Boursier,[§] Helen Flynn,[†] Anne M. Bouillot,[§] Paul Bamborough,[†] Jean-Marie G. Brusq,[§] Françoise J. Gellibert,[§] Emma J. Jones,[†] Alizon M. Riou,[§] Paul Homes,[†] Sandrine L. Martin,[§] Iain J. Uings,[†] Jérôme Toum,[§] Catherine A. Clément,[§] Anne-Bénédicte Boullay,[§] Rachel L. Grimley,[†] Florence M. Blandel,[§] Rab K. Prinjha,[†] Kevin Lee,[†] Jorge Kirilovsky,[§] and Edwige Nicodeme[§]

[†]Molecular Discovery Research, GlaxoSmithKline R&D, Stevenage SG5 4HT, U.K.

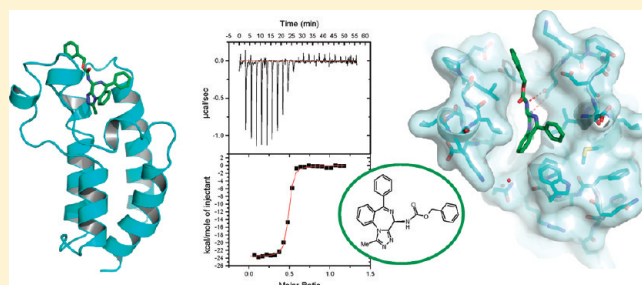
[†]Epinova, Discovery Performance Unit, GlaxoSmithKline R&D, Stevenage SG5 4HT, U.K.

[§]Lipid Metabolism Discovery Performance Unit, GlaxoSmithKline R&D, Les Ulis, France

S Supporting Information

ABSTRACT: Epigenetic mechanisms of gene regulation have a profound role in normal development and disease processes. An integral part of this mechanism occurs through lysine acetylation of histone tails which are recognized by bromodomains. While the biological and structural characterization of many bromodomain containing proteins has advanced considerably, the therapeutic tractability of this protein family is only now becoming understood. This paper describes the discovery and molecular characterization of potent (nM) small molecule inhibitors that disrupt the function of the BET family of bromodomains (Brd2, Brd3, and Brd4). By using a combination

of phenotypic screening, chemoproteomics, and biophysical studies, we have discovered that the protein–protein interactions between bromodomains and acetylated histones can be antagonized by selective small molecules that bind at the acetylated lysine recognition pocket. X-ray crystal structures of compounds bound into bromodomains of Brd2 and Brd4 elucidate the molecular interactions of binding and explain the precisely defined stereochemistry required for activity.



■ INTRODUCTION

Regulation of chromatin structure is a key mechanism by which a conserved genome can propagate distinct patterns of gene transcription and silencing across different cell lineages. This layer of epigenetic control is an important contributor to normal development but also plays a major role in the transformation events leading to tumorigenesis. Moreover, evidence is gradually emerging that dysregulation of epigenetic processes may be associated with the development of a range of human diseases, including cardiovascular disorders and autoimmunity.¹ Epigenetic information is encoded both by direct methylation of DNA at particular sites in the genome and by a series of post-translational marks placed on the tails of histone proteins which protrude from the nucleosome structure. These marks include methylation, acetylation, phosphorylation, and ubiquitination and are generated and erased by distinct families of enzymes which target a variety of residues on these histone tails.² The resulting pattern of modifications, or epigenetic code, is sensed by proteins that contain discrete “reader” modules, which are often found in combination to allow a complexity of permutations to be interpreted. These proteins then

assemble into complexes which can drive chromatin remodelling and result in transcriptional regulation.³

Significant progress has been made in the development of compounds that inhibit some of the enzymes responsible for the transfer of these epigenetic marks including the approval of Vorinostat (SAHA, a histone deacetylase inhibitor) for treatment of T-cell lymphomas.⁴ However, there are few available tools to modulate the many additional enzyme classes that mediate epigenetic changes (e.g., methyltransferases and demethylases) and fewer still for the wide variety of reader domains that exist (e.g., PHD, Tudor, Chromodomains, Bromodomains). Historical attempts to target protein–protein interactions, such as that described here between a reader protein and its chromatin partner, with potent and specific small molecule inhibitors, have proved challenging.^{5–7} On this basis, reader domains have until now been considered less viable opportunities for drug discovery.

Received: January 31, 2011

Published: May 13, 2011

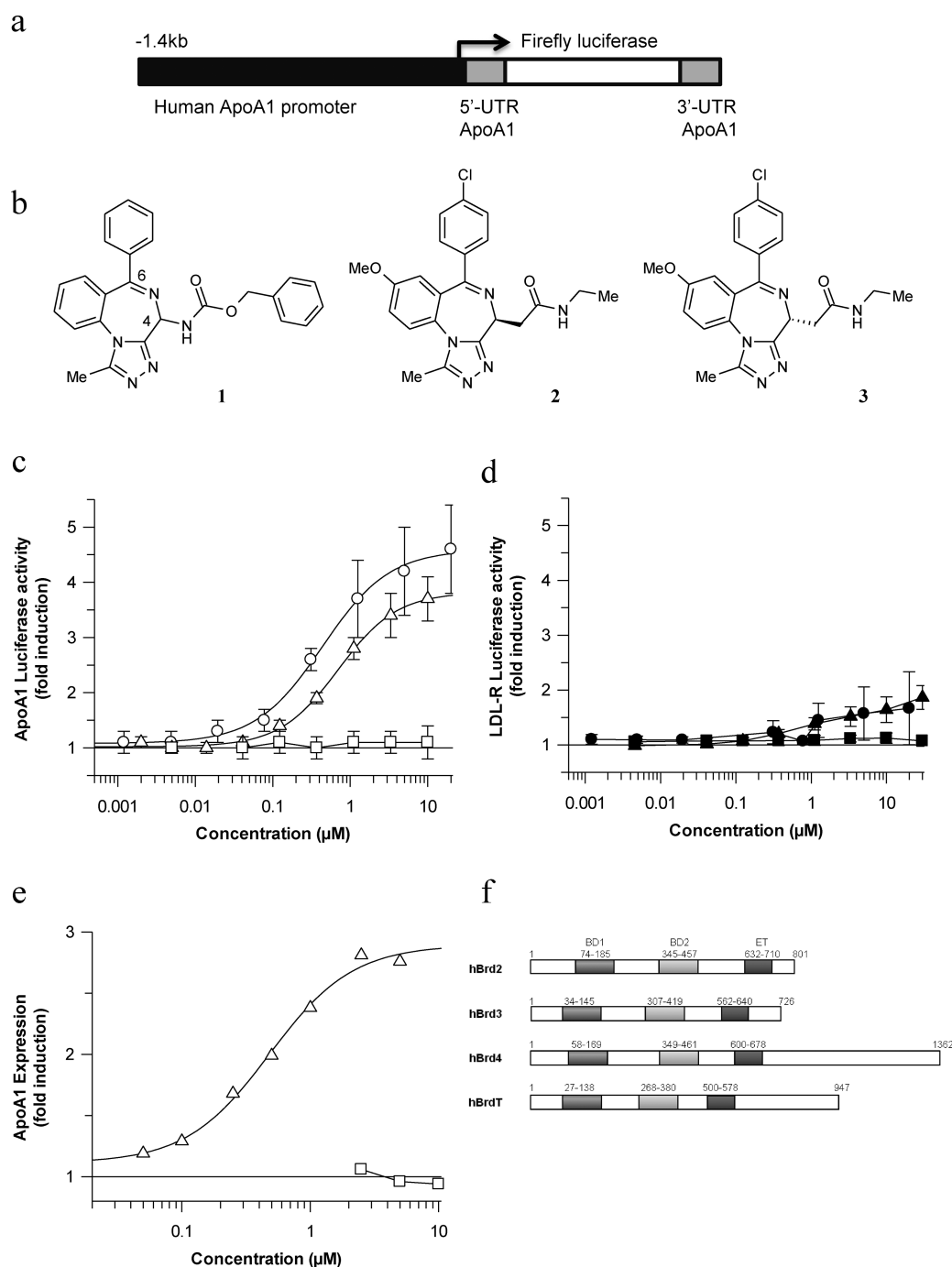
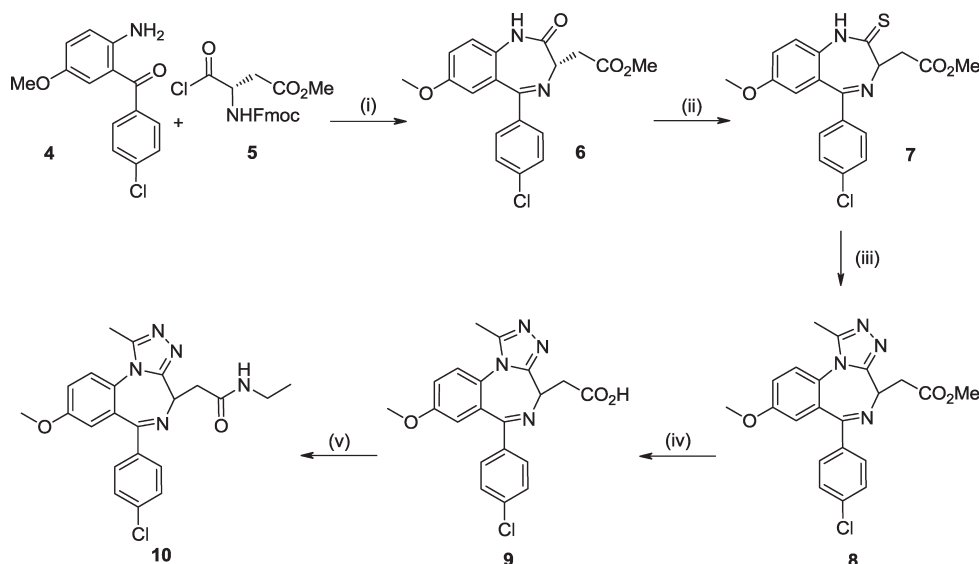


Figure 1. Luciferase reporter screen identifies small molecule inducers of ApoA1 expression. (a) The human ApoA1 promoter and 3'-UTR were cloned flanking a luciferase reporter gene and stably transfected into HepG2 cells. (b) High throughput screening identified a series of cell active small molecules and closely related inactive analogues. (c) Active compounds **1** (circles) and **2** (triangles) were able to dose-dependently increase the ApoA1 reporter gene (440 ± 60 and 700 ± 60 nM), whereas **3** (squares) failed to do so over the same concentration range. (d) All compounds had no effect on an analogous LDL-R reporter system showing the effects were specific for the ApoA1 gene. (e) The ability of **2** (triangles) to dose dependently increase Apo-A1 protein production in HepG2 cells is shown. The levels of secreted mature human ApoA1 protein were measured using ^{35}S pulse chase labeling in cells. The inactive enantiomer **3** has no effect even at the highest concentrations used. (squares) (f) The domain structure of Brd2, Brd3, Brd4, and BrdT, highlighting the tandem bromodomains BD1 and BD2 and the ET domain.

The use of cell-based reporter assays provides a means to identify chemical epigenetic modulators, as evidenced by a number of recent reports.^{8–10} An immense challenge for this approach is that once compounds have been discovered their molecular target or targets can be difficult to pinpoint, leading to compounds of unknown mode of action (MOA). This lack of

understanding limits their utility and confers risks associated with selectivity and safety as well as potential complexities in understanding the chemical structure activity relationships (SAR).

Apolipoprotein A1 (ApoA1) upregulation is associated with protection from atherosclerosis progression and with anti-inflammatory effects.¹¹ Despite much effort, no molecular mechanisms

Scheme 1. Synthetic Route^a

^a (i) (a) CHCl_3 , 60 °C, (b) Et_3N , DCM, reflux, (c) AcOH , 1,2-DCE, 60 °C; (ii) Lawesson's reagent, toluene, reflux; (iii) (a) $\text{H}_2\text{N}-\text{NH}_2$, THF, 0 °C, (b) Et_3N , AcCl , 0 °C to RT, (c) AcOH , THF, RT; (iv) NaOH , THF, RT; (v) ethylamine, HBTU, DIEA, THF, RT. **2** and **3** were obtained from **10** by chiral HPLC separation. For full details see Supporting Information, Figure S5a.

have yet been elucidated to suggest how this may be achieved in a therapeutic manner.¹² We therefore employed a “chemical genetic” approach using a reporter cell line to identify small molecules that were able to enhance ApoA1 expression. These upregulators specifically regulate the human ApoA1 gene but had an unknown mechanism of action.

In this manuscript, we describe the use of chemoproteomics, siRNA, biophysical assays and X-ray crystallography to elucidate the molecular target of these compounds and their MOA. The molecules inhibit the function of the tandem bromodomain containing family of transcriptional regulators known as the BET proteins¹³ (Brd2, Brd3, Brd4). They bind to the acetyllysine (AcK) recognition pocket and directly antagonize the interaction between the bromodomains and acetylated histone peptides. The liganded crystal structures presented here offer insights into how selectivity for the BET family is achieved and the basis of their mimicry of the native AcK peptide. This work has identified a novel class of chemical tools that can be used to modulate epigenetic processes and suggests that the protein–protein interactions mediated by bromodomains can be targeted therapeutically using small molecule antagonists.

RESULTS

Discovery of Small Molecule Upregulators of ApoA1 with Potent and Specific Effects. Efforts to target endogenous upregulation of ApoA1 expression are hampered by the absence of an obvious molecular mechanism around which to build a drug discovery effort. In 2001, we therefore generated a stable human HepG2 hepatocyte cell-line containing an ApoA1 luciferase reporter (Figure 1a) and used this to screen compounds in order to identify molecules with the ability to upregulate reporter gene activity. From this effort and with some minimal medicinal chemistry optimization,¹⁴ we identified the benzodiazepine (BZD) GW841819X¹⁵ (**1**, Figure 1b), which shows potent induction of the ApoA1 reporter gene with an EC_{50} of 440 nM and a maximum induction of 4.5-fold (Figure 1c). This compound

was a single enantiomer but of undefined chirality at the 4-position of the benzodiazepine (BZD) ring. To determine whether this was general transcriptional upregulation or a specific effect on the ApoA1 locus, we tested the compound's effect on an LDL-R promoter reporter construct in the same HepG2 cells. Compound **1** had very little effect on LDL-R luciferase activity at the concentrations at which it induces ApoA1 expression (Figure 1d), suggesting that the effect is indeed specific.

A program of medicinal chemistry was carried out to optimize the potency of **1** in the ApoA1 upregulation assay in the absence of any knowledge of the molecular target.¹⁴ While this is outside the scope of this manuscript, this work yielded much useful SAR, some of which it is now possible to rationalize using the X-ray structures presented here. For example, we found that the benzodiazepine core was essential for activity and the aryl group extending from the 6-position on the BZD ring was common to all active analogues.¹⁴ A variety of groups projecting from the 4-position of the BZD core were found to be well tolerated and could be used to modify the physicochemical and pharmacokinetic properties of the molecules. This led to the synthesis of GSK525762A¹⁵ (**2**, Figure 1b; Scheme 1), which shows similar potency and specificity to **1** in the reporter gene systems (Figure 1c, d; EC_{50} 700 nM) but whose properties make it more suitable for in vivo experiments.^{14,15} Intriguingly, activity was found to depend critically upon the stereochemistry at the 4-position. Thus, the *R*-enantiomer of **2**, GSK525768A¹⁵ (**3**, Figure 1b), is unable to alter reporter gene activity (Figure 1c). The activity of the BZDs was not limited to reporter gene assays, as **2** displayed a similar upregulation of endogenous ApoA1 expression levels in HepG2 cells (as quantified by ³⁵S pulse chase labeling of secreted protein in HepG2 cells). In these studies, **3** was also found to be inactive (Figure 1e). This dependence on stereochemistry strongly implied that the observed activity resulted from specific interactions with defined but unknown molecular targets.

To try to identify these targets, a panel of structurally related compounds that spanned a full range of activities in the luciferase

assay (from nM to inactive) were profiled against panels of kinases, ion channels, nuclear receptors, GPCRs, and other drug-target protein classes.¹⁵ This exercise did not provide any insights into the mode of action of these compounds beyond suggesting that these compounds may act through a novel class of targets not represented in our panels.

BZD Compounds Bind to the Tandem Bromodomains of Brd2,3,4 of the BET Protein Family. Recognizing that the target for our compounds was probably not among the established drug classes, we embarked upon a chemoproteomics approach. Briefly, we generated an affinity matrix by linking a derivatized version of **2** to a ReactiGel matrix (“active BZD matrix”, see Supporting Information, Section 4). A control matrix using an inactive BZD analogue was also generated. We then performed affinity chromatography by passing lysates from HepG2 cells over the affinity matrix, followed by extensive washing. A consistent and defined pattern of proteins were retained by the active BZD matrix but were absent when the inactive BZD matrix or matrix alone was used (Supporting Information, Figure 4i,ii (S7–S10)). The binding of these proteins to the active BZD matrix could be competed away by the addition of excess **1** (100 μ M) but was not altered by the inclusion of DMSO or an inactive analogue. Thus it appeared that the proteins retained on the active matrix represent specific protein targets of the BZD compounds. Mass spectrometric analysis of all the proteins retained by the active matrix by LC/MS/MS reproducibly identified them as fragment peptides from just three proteins, namely Brd2, Brd3, and Brd4, with sufficient coverage to allow definitive identification (see Supporting Information, Section 4 (S7–S19)).

These proteins belong to the BET family of transcriptional coregulators, which share a characteristic architecture of a tandem bromodomain motif at the N-terminus and an “extra-terminal” (ET) domain at the C-terminus (Figure 1f). A fourth member of this family, BrdT, has also been previously described, but whereas Brd2, Brd3, and Brd4 are all ubiquitously expressed, BrdT is only expressed in testis¹⁶ and is therefore not present in HepG2 cells. No other proteins were detected on the gels, implying that the BET family of proteins may be the molecular targets for the BZD compounds.

The N and C-terminal regions of BET proteins have distinct functions.^{13,17} The N-terminal tandem bromodomains (BD12) recognize patterns of acetylated lysines on histone tails, allowing the specific localization of the BET proteins to defined areas of chromatin. The C-terminal ET domain is thought to be involved in scaffolding the multiprotein complexes associated with the BET proteins to bring about transcriptional regulation. To define more precisely the region(s) of the BET proteins involved in compound binding, Flag-tagged Brd2 cDNA constructs of full length Brd2(1–801) or N(1–473) and C(473–801) terminal truncates (Supporting Information, Figure 4i(b)) were generated and transiently transfected into HepG2 cells. Although all three proteins could be recovered by immunoprecipitation using an anti-Flag antibody, affinity purification of the same lysates using the active BZD matrix recovered only the full length and N-terminal region of Brd2 and not the C-terminal domain construct (Supporting Information, Figure 4i(c) (S7–S10)). Therefore, the BZD compounds interact with the BET proteins via their bromodomain-containing N-terminal region.

BZD Compounds Bind Stoichiometrically to Each BET Bromodomain with nM Potency and Can Bind the Tandem Bromodomain at Two Sites Simultaneously. To determine the specificity and nature of the BZD binding to the BET

proteins, biophysical and structural methods were employed. Initially, the N-terminal portions of Brd2, Brd3 and Brd4 containing both bromodomains (BD12) were expressed in *E. coli* and purified to homogeneity (Supporting Information, Figure 5i (S22)). Isothermal titration calorimetry (ITC) experiments confirmed a direct and specific high affinity (19–80 nM) interaction of **1** with the tandem bromodomains of the BET family (Figure 2a, Supporting Information, Figure 5ii (S23)). Interestingly, it appears that two molecules of **1** bind to each molecule of the BET BD12 protein. This unexpected stoichiometry indicates that compounds may bind to a shared motif within each bromodomain and can bind simultaneously to multiple bromodomains when present in a single protein. To confirm this, constructs expressing each bromodomain of Brd2 were generated separately and the proteins purified (Supporting Information, Figure 5i (S22)). Compound **1** bound to both the individual BD1 and BD2 domains with a 1:1 stoichiometry with very similar affinities, 46 and 52.5 nM, respectively (Figure 2b,c). The thermodynamic parameters of this binding are given in Figure 2d. This provides compelling evidence that the BZD compounds recognize a common feature of the two bromodomains.

The behavior of the single bromodomains of Brd2 was further investigated using surface plasmon resonance (SPR) at 25 °C. Titrations of **1** over immobilized Brd2-BD1 (Figure 2e) and Brd2-BD2 (Figure 2f) gave dissociation constants of 220 and 54 nM, respectively. These affinities are broadly consistent with the ITC findings and therefore support the observation of specific interaction of **1** with BET bromodomains using an orthogonal method. The approximately 5-fold weaker affinity to Brd-BD1 at 25 °C measured by SPR (220 nM) compared to that found at 16 °C by ITC (46 nM) is believed to be a real and significant difference and due to a strong temperature dependence in the K_D for BD1 binding. This was also observed during the ITC experiments and led to the Brd2-BD1 titration being carried out at 16 °C rather than 26 °C as a marked reduction in binding enthalpy and affinity was seen at 26 °C (Supporting Information, Figure 5ii (S23)).

The binding kinetics of **1** to Brd2-BD1 are also noticeably more rapid than seen for Brd2-BD2 (Figure 2e,f). It is tempting to speculate that these differences may translate to the possibility of sequential and cooperative binding to the individual sites in tandem domain constructs. However, our experience and the emerging literature on other epigenetic targets suggests that the presence or absence of adjacent domains can have a profound influence on the activity, kinetics, specificity, and function of truncated proteins¹⁸ and it may be difficult to extrapolate the behavior of truncates to full length proteins with high fidelity.

As bromodomains are known to bind to lysine-acetylated histone peptides and to function as transcriptional regulators,^{19,20} we tested the ability of BZD compounds to modulate the interaction of a tetra-acetylated lysine histone 4 peptide (H4AcK₄) with recombinant tandem constructs of Brd2, 3, and 4 in a FRET assay (Figure 2g,i). The active exemplar compounds exhibit dose dependent inhibition of peptide binding to the Brd2, 3, and 4 proteins with IC₅₀s of between 15 and 30 nM (Figure 2j). These compounds therefore function as antagonists of the BET proteins' role as sensors of histone acetylation.

Crystallography Shows that BZDs are Orthosteric Antagonists Acting at the AcK Recognition Site. To determine whether compounds act by direct steric competition with the H4AcK₄ peptide or by an indirect allosteric mechanism, structures of BZD compounds complexed with BD1 and BD2 single bromodomains of the BET family were determined by X-ray crystallography (see Supporting Information, Section 7). Figure 3

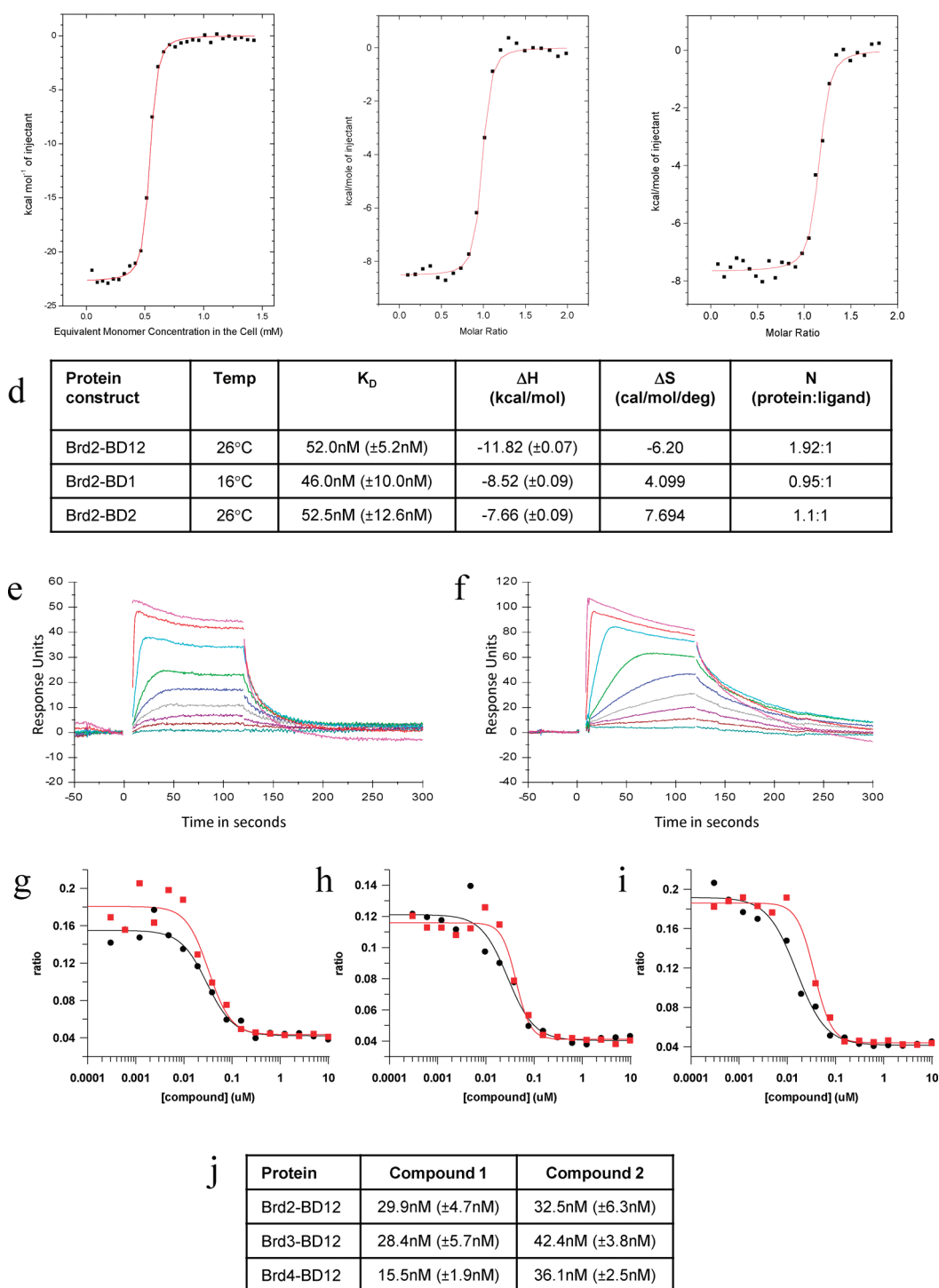


Figure 2. Biophysical data for BZD binding to BET proteins. Isothermal calorimetric titration curves and analysis for the titration of solutions of (a) Brd2-BD12, (b) Brd2-BD1, and (c) Brd2-BD2 into compound 1, demonstrating stoichiometric binding of one compound per bromodomain present in the protein. (d) The thermodynamic parameters of 1 binding to the Brd2 constructs. SPR sensorgrams of 1 injected over (e) Brd2-BD1 ($K_D = 220 \pm 50$ nM ($n = 4$)). (f) Brd2-BD2 ($K_D = 54 \pm 14$ nM ($n = 3$)) at tripling dilutions start at $6.7 \mu\text{M}$, illustrating the difference in the kinetics of binding to the two domains. The ability of 1 (black) and 2 (red) to dose-dependently displace a tetra-acetylated H4 peptide from the tandem BET bromodomains of (g) Brd2, (h) Brd3, and (i) Brd4 in the FRET assay with potencies in the 15–40 nM range (j).

shows structures of 1 with Brd4-BD1/2, as well as 1 and 2 with Brd2-BD1.

The BET bromodomains adopt a left-handed four-helix bundle topology consistent with other members of the bromodomain superfamily.^{21,22} Structures of BET family members in

complex with acetylated lysine-containing peptides have been determined crystallographically by several groups. These include Brd2-BD1/BD2,²³ Brd4-BD1,²⁴ and BrdT-BD1/BD2.²⁵ These studies have shown that the acetylated lysine occupies a pocket formed by the ZA and BC loops at one end of the helical bundle

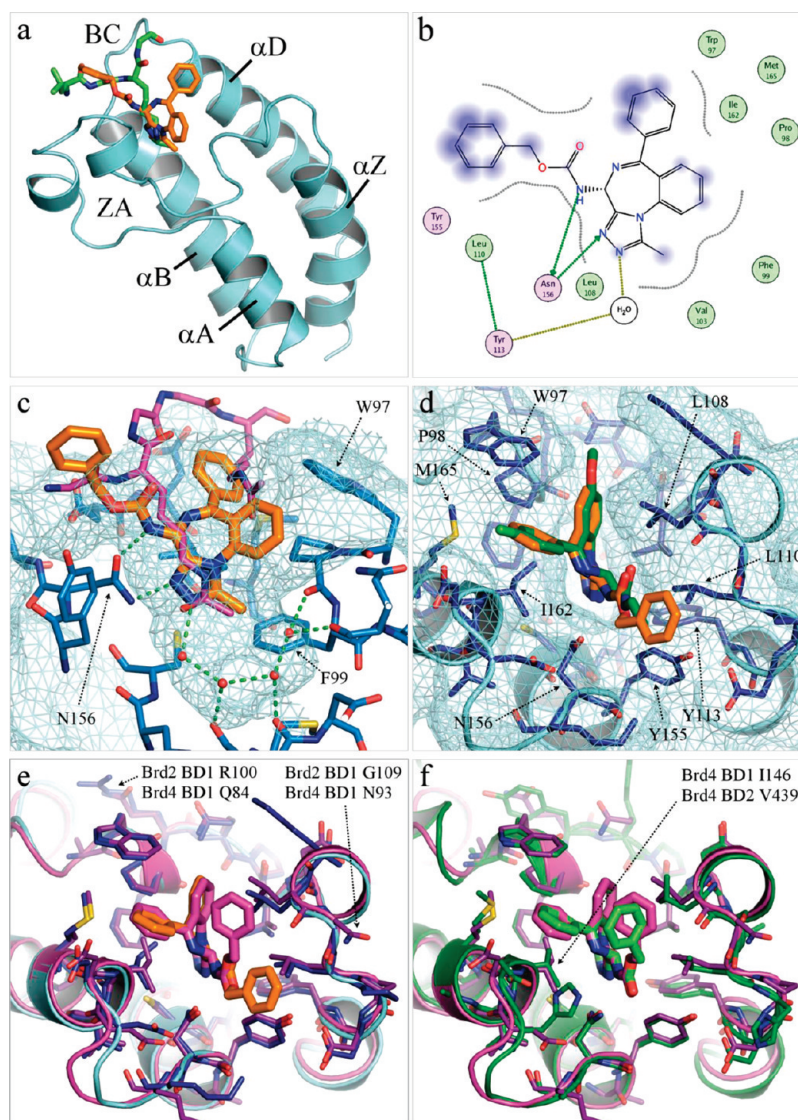


Figure 3. Molecular interactions of BZD with BET bromodomains. (a) The four-helix bundle topology of Brd2-BD1 complexed with **1** (orange). The acetyl-lysine K12Ac histone H4 peptide taken from its complex with Brd2 (PDB entry 2DVQ²³) is shown in green. (b) Schematic showing the interactions between **1**, the Brd2-BD1 site and nearby water molecules. (c) Brd2-BD1 (blue) complexed with **1** (orange), superimposed on the diacetylated K5Ac K8Ac histone H4 peptide (magenta) taken from BrdT-BD1/H4K5AcK8ac complex (PDB entry 2WP2²⁵). In this figure and in Figure 4d, the surface of the protein is shown as a blue mesh. In Figure 4c, a view through the protein enables the shape of the AcK pocket to be clearly delineated and the conserved waters lining the bottom and their extensive hydrogen bonding network to be visualized. (d) Brd2-BD1 (blue) complexed with **1** (orange) and **2** (green) showing the similar binding modes of the two compounds. This is a view from above the protein surface down into the AcK pocket. (e) Superimposed complexes of **1** bound into Brd2-BD1 (blue, with **1** in orange) and Brd4-BD1 (magenta). The two amino acid substitutions in the shell of residues surrounding the binding site (labeled) do not significantly alter the binding mode of the compound to the BD1 domains of the two proteins. This again is a view from above the protein surface down into the AcK pocket, in an identical manner to 4d and 4f. (f) Superimposed complexes of **1** bound into Brd4-BD1 (magenta) and Brd4-BD2 (green), viewed from above the AcK pocket, showing the similar binding modes of the compound to the two bromodomains of Brd4. This is unaffected by the conservative substitutions within the binding site, such as that of the gatekeeper residue (labeled).

(Figure 3a). The acetyl group on the AcK side chain interacts with a network of water molecules located at the bottom of the pocket that participate in a hydrogen-bonding network with the asparagine and tyrosine residues that are conserved in the majority of the bromodomains (Figures 3c and 4a). These residues are essential to the bromodomains' function of "reading" the presence of the acetyl-lysine modification.

The BZD compounds bind to the acetyl-lysine recognition pocket (Figure 3a, 3b) and interact with the same conserved water

network, which is maintained with little variation in over a hundred structures we have determined to date. To explain the features of compound binding it is instructive to compare the BZD complexes with the crystal structure of a histone peptide, for example, as in Figure 3c, which shows an overlay of Brd2-BD1 bromodomain bound to **1** (orange) on the diacetylated H4 peptide (magenta) from a published structure.²⁵ The methyl group of **1** binds into the small hydrophobic pocket that is responsible for recognition of the methyl group of the acetyl headgroup of the acetyl-lysine. This is formed in

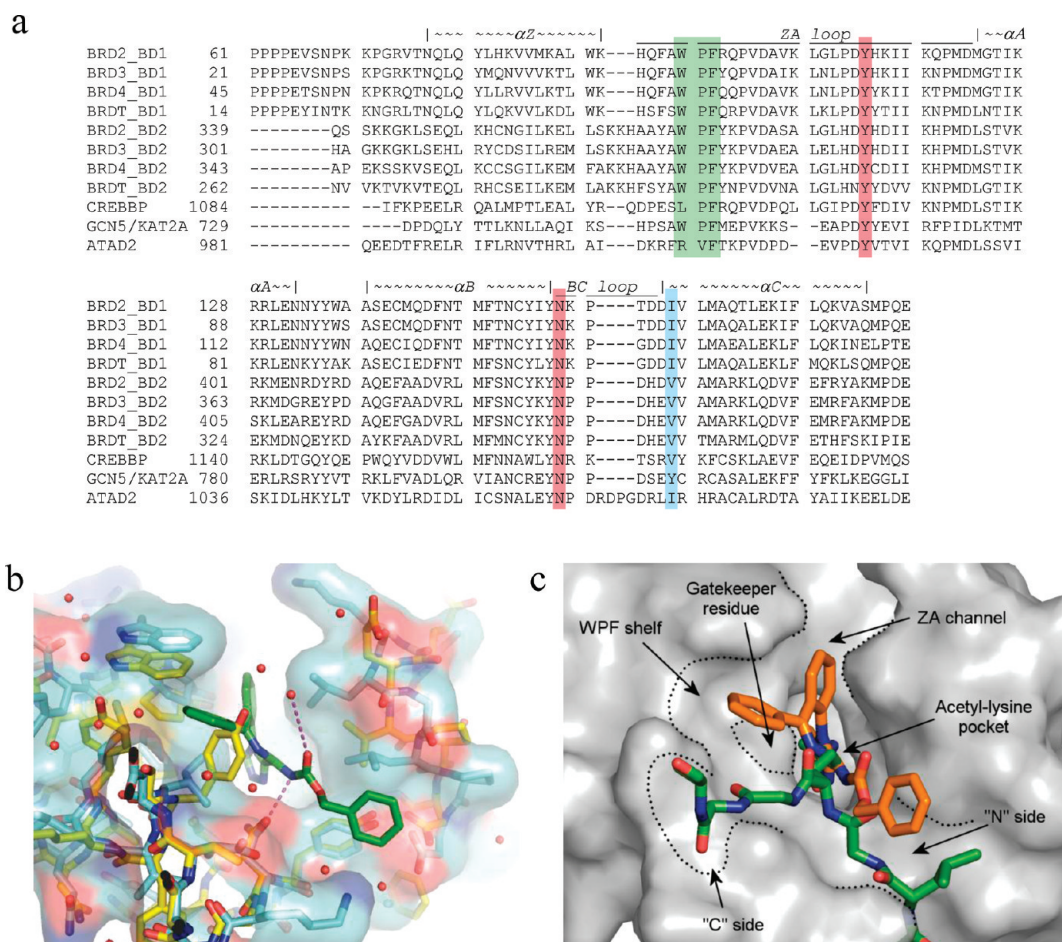


Figure 4. Basis of BZD selectivity among bromodomains. (a) Multiple sequence alignment of human BET Brd2, 3, 4, and T bromodomains with GCN5. Highlighted in blue is the I/V to Y sequence difference in the gatekeeper residue at the bottom of the WPF shelf observed between BD1, BD2, and GCN5, respectively. The WPF motif is highlighted in green, and the conserved tyrosine and asparagine that are key to acetylated lysine recognition are highlighted in red. (b) The X-ray structure of Brd2-BD1 (blue stick and surface) with **1** (green stick) has been overlaid with GCN5 (PDB entry 1E61 as yellow stick).²⁵ This illustrates that the change of the gatekeeper residue from isoleucine to tyrosine would likely obstruct the entrance of the WPF shelf. (c) A surface representation of Brd2-BD1 with **1** (orange stick), overlaid with the acetylated H4 peptide from the PDB entry 2DVQ shown in green. The accessible areas for ligand binding outside of the conserved acetylated lysine (AcK) binding site are mapped out in this diagram. The N-terminal portion of the peptide binds in the N-side before the AcK and then exits to make interactions along the C-side. **1** also accesses the N-side but explores additional interactions in the WPF shelf and the ZA channel.

large part by the side chain of Phe99 in Brd2-BD1, which is perfectly conserved in the other BET bromodomains (Figure 4a).

The two nitrogen atoms of the 1,2,4-triazolyl ring of the BZD together mimic the carboxyl group of the acetyl headgroup. One ring nitrogen (N1) accepts a hydrogen-bond from the water molecule that bridges to the hydroxyl group of the side chain of the conserved tyrosine residue (position 113 in Brd2-BD1). The second nitrogen (N2) accepts a hydrogen bond from the side chain NH₂ group of the conserved asparagine (position 156 in Brd2-BD1). The ability of a triazolyl ring to mimic the acetyl group in this way was unexpected, but this discovery was important because it suggested for the first time that other diverse chemotypes can act as antagonists of the bromodomain/AcK peptide interaction.

The fused phenyl ring of the benzodiazepine core of **1** extends beyond the region occupied by the histone peptide, binding into a lipophilic pocket we termed the ZA channel (Figure 4b), sandwiched between side chains of the long ZA loop (notably Pro98 and Leu108 in Brd2-BD1). The curvature of the benzodiazepine is well matched to the shape of the channel, providing

good shape complementarity which may in part explain the high binding potency of these compounds.

The pendent phenyl group at the 6-position of the benzodiazepine interacts with another hydrophobic region of the BC loop that we have named the WPF shelf (because it includes the conserved WPF motif present in all of the BET family bromodomains), especially residues Trp97 and Pro98 of Brd2-BD1. Other Brd2-BD1 residues that make up the WPF shelf include Ile162 and Met165. While this manuscript was in preparation, a report was published that described the X-ray structures of BD1 and BD2 bromodomains from BrdT in complex with histone peptides from H4 and H3, respectively.²⁵ One key finding of Moriniere et al.²⁵ was the binding mode of a diacetylated histone H4 tail to the single bromodomain of BrdT-BD1, in which the established AcK pocket binds the first H4AcK mark at position 5. Interestingly, the second AcK at position 8 lies within the WPF shelf region of the binding site. The C_γ–C_ε atoms of the H4AcK8 side chain overlay closely with the positions of the pendant phenyl ring of the BZD compounds (Figure 3c). This reinforces

our hypothesis that occupation of the WPF shelf and surrounding regions of the site are critical for binding and for governing selectivity. It seems that the BZD compounds serendipitously identified an important hotspot for specific bromodomain recognition.

The crystal structure clearly shows that the R-enantiomer of **1** binds to the bromodomain. This stereocenter is the position from which the benzyl carbamate moiety projects and which was found to be key for Apo-A1 activity. This carbamate group is mobile, as evidenced by its high B-factors and variable positions in different molecules within the asymmetric unit, but it extends into the volume that is occupied by the peptide chain of the AcK (or the “N-side”) (Figure 3c). The NH group of the carbamate acts as an additional hydrogen-bond donor to the side chain of Asn156, which is an interaction that is not made by the AcK peptide. This partially explains the reduced activity of one enantiomer of the BZD compounds, which would be unable to make this interaction. However, a more significant reason for their inability to bind is that they would clash sterically with the side of the pocket, particularly the side chains of Leu108 and Leu110.

Other members of the BZD class of compounds bind to Brd2-BD1 with essentially identical binding modes for their BZD core, as shown for **2** bound to Brd2-BD1. The superimposition of **1** and **2** is shown in a different orientation in Figure 3d. The change from the carbamate linker in the 4-position of **1** to an amide in **2** results in the loss of a direct H-bond with Asn156, but this is replaced with a water mediated interaction between the amide and N156.

To clarify the way in which these compounds bind to other members of the BET family, crystal structure complexes with these bromodomains were also determined. For example, the structure of **1** with Brd4-BD1 (Figure 3e) shows essentially identical binding interactions to Brd2-BD1. This is not surprising, given the relatively high conservation of the active sites between the BD1 domains of the BET family. The different positions of the benzyl carbamate substituent visible in Figure 3e reflect its mobility, consistent with the ability to tolerate modification at this position as discussed above. The second BD2 bromodomains are more distantly related to the BD1s (Figure 4a). Despite this, BZD compounds bind to the BD2 domains in a similar manner, as is shown by the complex between **1** and Brd4-BD2 (Figure 3f). This observation is consistent with the similar experimental binding affinities described earlier.

The complex structures explain the SAR observed within the BZD series and rationalize the potent nM affinity of these compounds, as well as the tight requirement for the appropriate enantiomer within the series. They also elucidate the mode of action of these compounds: they directly antagonize the pivotal recognition of acetylated lysine peptides by BET family bromodomains and thus influence transcriptional regulation and chromatin remodelling.

ApoA1 Upregulation Can Be Induced by siRNA Knockdown of Brd4. Our experiments established the BZD compounds as inhibitors of the BET proteins, but to confirm that this function was responsible for the upregulation of ApoA1, we conducted siRNA studies. As previously observed, treatment of HepG2 cells with 1 μ M **1** was able to induce ApoA1 mRNA expression by approximately 3-fold (Figure 1e and Supporting Information (S6–S8, S20–S21)). Treatment of HepG2 cells with siRNA designed to give specific knockdown of Brd2 and Brd3 had no effect on ApoA1 expression, whereas progressive knockdown of Brd4 expression resulted in a gradual and signifi-

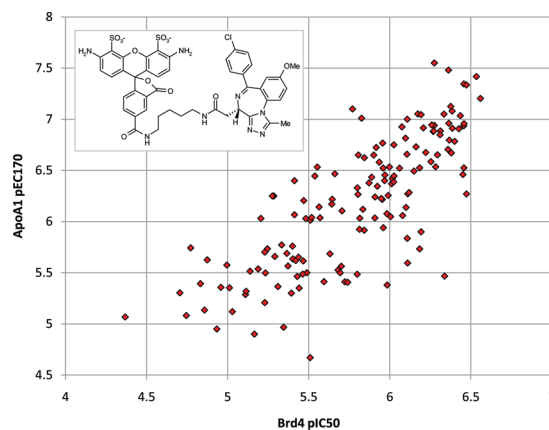


Figure 5. Cellular ApoA1 upregulation correlates with in vitro binding affinity to BET proteins. Plot of mean Apo-A1 HepG2 upregulation pEC_{170} against Brd4 fluorescence anisotropy pIC_{50} , for 150 BZD compounds tested in both assays, showing excellent correlation. Data for Brd2 and Brd3 are shown in Supporting Information, Figure 6i (S31).

cant increase in ApoA1 protein. (Supporting Information, Figure 4i (S7), S20–S21). These data clearly suggest that upregulation of ApoA1 can be driven by disrupting the bromodomain binding function of Brd4. However, as only mRNA was monitored the roles of Brd2 and Brd3 in Apo-A1 regulation cannot be ruled out, either individually or in combination with each other and Brd4.

Cellular ApoA1 Upregulation Strongly Correlates with In Vitro Affinity to BET Proteins. The knowledge that **2** is a potent ligand for the BET bromodomains, and awareness of the SAR surrounding this ligand allowed an active fluorescent derivative to be made and a fluorescent anisotropy (FA) displacement assay to be established (Supporting Information, Section 6 (S31–S33)). The results of profiling 150 compounds from the benzodiazepine series with a broad range of ApoA1 activities in this in vitro binding assay are given in Figure 5 (also see Supporting Information, Figure S6i (S31)). The correlation between Brd2, 3, and 4 binding affinity and ApoA1 upregulation is excellent ($R = 0.75, 0.76,$ and 0.78 respectively). This further supports the siRNA findings that BET-histone inhibition results in ApoA1 upregulation.

DISCUSSION AND CONCLUSION

In this paper, we described how we used a reporter assay to identify a novel class of ApoA1 upregulators (BZDs) and epigenetic “reader” inhibitors. The mode of action of these compounds has been deconvoluted by chemoproteomics and biophysical experiments to demonstrate unequivocally that they act as direct functional antagonists of AcK histone binding to the BET family of bromodomains. Our compounds are pan-BET active, and therefore we cannot specify whether inhibition of one or all of these proteins are required for the Apo-A1 activation for which they were originally discovered. However, the siRNA studies suggests at least a previously unknown association of Brd4 with ApoA1 regulation.

While significant progress has been made in the area of epigenetics through the use of gene knockout mice, siRNA knockdown, or overexpression of domain deletions, these studies are generally unable to define the contribution of each individual domain to the overall function of the protein. The BZD

compounds provide a unique opportunity to do so for BET bromodomains.

There have been some notable previous attempts to find small molecule inhibitors of bromodomains^{6,7} using a structure-based design approach, especially targeting the bromodomains of PCAF and CREBBP. These efforts have successfully identified compounds of affinities in the μM or greater range. While these affinities are comparable to those often measured between isolated bromodomains and their histone partners, the ability to use micromolar compounds in chemical biological studies can be limited. The BZD compounds reported here represent a novel chemical template, distinct from the previously reported simple acetyl containing templates, with clear mode of action, and demonstrate the ability to produce inhibitors with high (nM) affinity and cell permeability.

The biological role and therapeutic potential of the BET proteins is beginning to emerge in the literature. Key observations of their importance in viral segregation²⁶ and B-cell lymphomagenesis²⁷ suggest that our compounds may have potential in these antiviral and oncology indications, respectively. Two recent publications also highlight the potential benefits of BET BZD inhibitors for both anti-inflammatory diseases and a specific midline carcinoma.^{15,28}

The BZDs bind to both BD1 and BD2 bromodomains of the BET family with comparable affinity. However, the affinity purification studies identified only the BET family of proteins as BZD binders despite the likely presence of many other bromodomain containing proteins in cell lysates. We hypothesize that BET family specificity is achieved by making distinct contacts outside the acetyl-lysine cavity with the BC and ZA loops, which are known to differ significantly in both composition and length between bromodomain containing proteins.²¹ This hypothesis is strengthened by the inability to detect an interaction between **1** and two bromodomains, which differ in the length and characteristics of the ZA and BC loops, CREBBP and ATAD2 (Figure 4a), suggesting affinities in excess of 50 μM (Supporting Information, Figure SIV.v (S25–S26)). This is supported by recent data on related compounds and their selectivity for the BET proteins.^{15,28}

In contrast, differences in these loop regions between the BET domains are relatively minor and are tolerated by the BZD compounds. For example, BD1 of Brd2, **3**, and **4** have an isoleucine at the position analogous to residue 162 in Brd2. This “gatekeeper” residue is located at the entrance to the WPF shelf. The BD2 domains of the BET family have a conservative replacement of this residue by valine (as shown in Figure 3f and Figure 4a) which is also well tolerated. CREBBP and ATAD2 also have small gatekeeper residues of valine and isoleucine, respectively, but this is not the case for all bromodomains as the structure of closely related bromodomain such as GCN5²⁹ (Figure 4a) shows. In this bromodomain, the gatekeeper is a much larger tyrosine residue. This bulky residue would be expected to hinder access to the WPF shelf, and thus clash with the binding of the pendent benzyl of a BZD compound (Figure 4b).

The crystal structures of several BZDs with a number of BET bromodomains described in this paper yield insights into the molecular mimicry of the acetylated-lysine interactions. They suggest opportunities to exploit commonalities and differences in the bromodomain family to design compounds that achieve distinct profiles of inhibition. This is likely to be an important requirement for not only therapeutic indications but also for obtaining chemical tools that will help to dissect the complex role of these epigenetic targets.

Similarly, small molecule inhibitors of other domains will provide powerful tools to understand the contributions of the

“reader” domains in control of epigenetic processes in a way not currently possible using siRNA or knockout strategies. The knowledge generated using such compounds will undoubtedly unravel many of the complex processes regulating transcription in health and disease.

In conclusion we present the discovery of a class of potent compounds with a novel epigenetic mechanism, extending the druggable genome to include bromodomains.

METHODS

Chemistry. *General.* All commercial chemicals and solvents are reagent grade and were used without further purification unless otherwise specified. All reactions except those in aqueous media were carried out with the use of standard techniques for the exclusion of moisture. Reactions were monitored by thin-layer chromatography on 0.2 mm silica gel plates (ALUGRAM SIL G/UV254, Macherey-Nagel) and visualized with UV light. Final compounds were typically purified either by flash chromatography on silica gel (E. Merck, 40–63 mm) or by recrystallization. ¹H and ¹³C NMR spectra were recorded on a Bruker 300 MHz Avance DPX. Chemical shifts are reported in parts per million (ppm, δ units). Splitting patterns are designed as s, singlet; d, doublet; t, triplet; q, quartet; m, multiplet; bs, broad singlet. High-resolution mass spectra were recorded on a Micromass LCT (TOF) spectrometer coupled to an analytical high performance liquid chromatography (HPLC) was conducted on a XTERRA-MS C18 column (30 mm \times 3 mm id, 2.5 μm) eluting with 0.01 M ammonium acetate in water and 100% acetonitrile (CH₃CN), using the following elution gradient: 0–100% CH₃CN over 4 min and 100% CH₃CN over 1 min at 1.1 mL/min at 40 °C. Mass spectra were acquired in either positive or negative ion mode under electrospray ionization (ESI) method. Specific rotations were measured on a Perkin-Elmer 343 polarimeter. The purity of all compounds were >95% as judged by LC-MS and NMR.

Compound 2 2-[(4S)-6-(4-Chlorophenyl)-1-methyl-8-(methoxy)-4H-[1,2,4]triazolo[4,3-a][1,4]benzodiazepin-4-yl]-N-ethylacetamide and *Compound 3* 2-[(4R)-6-(4-Chlorophenyl)-1-methyl-8-(methoxy)-4H-[1,2,4]triazolo[4,3-a][1,4]benzodiazepin-4-yl]-N-ethylacetamide. These were prepared by chiral separation of compound **10**. The racemic mixture of 2-[(4-chlorophenyl)-1-methyl-8-(methoxy)-4H-[1,2,4]triazolo[4,3-a][1,4]benzodiazepin-4-yl]-N-ethylacetamide **10** (200 mg) was separated by HPLC using a ChiralPack AD (250 mm \times 20 mm id, 10 μm) column eluting with EtOH/hexane (60/40) as the mobile phase (flow rate: 17 mL/min). **2** eluted at 5.21 min as the first peak. $[\alpha]_D^{20} = +88.1$ ($c = 1.0015/\text{MeOH}$). **3** came off at 24.28 min. $[\alpha]_D^{20} = -87.7$ ($c = 1.0015/\text{MeOH}$). **3** came off at 24.28 min. $[\alpha]_D^{20} = -87.7$ ($c = 1.0015/\text{MeOH}$).

Compound 10 2-[6-(4-Chlorophenyl)-1-methyl-8-(methoxy)-4H-[1,2,4]triazolo[4,3-a][1,4]benzodiazepin-4-yl]-N-ethylacetamide. To a solution of acid **9** (4.5 g, 11.4 mmol) in THF at RT was added diisopropylethylamine DIEA (4 mL, 22.7 mmol, 2 equiv), followed by HBTU (8.6 g, 22.7 mmol, 2 equiv). The reaction mixture was stirred for 3 h at this temperature, and ethylamine (11.3 mL, 2 M in THF, 22.7 mmol, 2 equiv) was added dropwise. The mixture was stirred overnight before being concentrated under reduced pressure. The crude material was dissolved in DCM and washed successively with water, 1N NaOH and 1N HCl. The organic layer was dried over Na₂SO₄, filtered, and concentrated in vacuo. The crude solid was recrystallized in CH₃CN to give the title compound **10** (4.1 g, 85% yield) as a white solid. Yield from **9**: 85%, white solid. $R_f = 0.48$ (DCM/MeOH:90/10); mp 140–145 °C. ¹H NMR (300 MHz, CDCl₃) δ 7.53–7.47 (m, 2H), 7.39 (d, $J = 8.9$ Hz, 1H), 7.37–7.31 (m, 2H), 7.20 (dd, $J = 2.9$ and 8.9 Hz, 1H), 6.86 (d, $J = 2.9$ Hz, 1H), 6.40 (m, 1H), 4.62 (m, 1H), 3.80 (s, 3H), 3.51 (dd, $J = 7.3$ and 14.1 Hz, 1H), 3.46–3.21 (m, 3H), 2.62 (s, 3H), 1.19 (t, $J = 7.3$ Hz, 3H). ¹³C NMR (75 MHz, DMSO-*d*₆)

δ 169.2, 165.5, 157.4, 155.8, 150.7, 137.3, 135.4, 131.0, 129.3, 128.2, 126.4, 125.6, 117.8, 115.1, 55.8, 53.3, 37.6, 33.4, 14.8, 11.5. HRMS (M + H)⁺ calcd for C₂₂H₂₃³⁵ClN₃O₂ 424.1540; found 424.1525.

Compound 9 [6-(4-Chlorophenyl)-1-methyl-8-(methoxy)-4H-[1,2,4]triazolo[4,3-a][1,4] benzodiazepin-4-yl] Acetic Acid. To a solution of ester **8** (7.4 g, 18.1 mmol) in THF (130 mL) at RT was added 1N NaOH (36.2 mL, 36.2 mmol, 2 equiv). The reaction mixture was stirred at this temperature for 5 h before being quenched with 1N HCl (36.2 mL) and concentrated in vacuo. Water is then added and the aqueous layer was extracted with DCM (3×), and the combined organic layers were dried over Na₂SO₄, filtered, and concentrated under reduced pressure to give the title compound **9** (7 g, 98% yield) as a pale-yellow solid. Yield from **8**: 98%, pale-yellow solid. ¹H NMR (300 MHz, CDCl₃) δ 7.55–7.48 (m, 2H), 7.41 (d, *J* = 8.9 Hz, 1H), 7.38–7.31 (m, 2H), 7.22 (dd, *J* = 2.9 and 8.9 Hz, 1H), 6.90 (d, *J* = 2.9 Hz, 1H), 4.59 (dd, *J* = 6.9 and 6.9 Hz, 1H), 3.81 (s, 3H), 3.70 (dd, *J* = 6.9 and 25.7 Hz, 1H), 3.61 (dd, *J* = 6.9 and 25.7 Hz, 1H), 2.63 (s, 3H). ¹³C NMR (75 MHz, DMSO-*d*₆) δ 172.1, 165.6, 157.4, 155.5, 150.8, 137.2, 135.4, 131.1, 129.2, 128.3, 126.3, 125.6, 117.9, 115.2, 55.8, 52.9, 36.5, 11.5. HRMS (M + H)⁺ calcd for C₂₀H₁₈³⁵ClN₄O₃ 397.1067; found 397.1063.

Compound 8 Methyl [6-(4-Chlorophenyl)-1-methyl-8-(methoxy)-4H-[1,2,4]triazolo[4,3-a][1,4]benzodiazepin-4-yl]acetate. Yield from **7**: 91%. ¹H NMR (300 MHz, CDCl₃) δ 7.54–7.47 (m, 2H), 7.40 (d, *J* = 8.8 Hz, 1H), 7.37–7.31 (m, 2H), 7.22 (dd, *J* = 2.8 and 8.8 Hz, 1H), 6.89 (d, *J* = 2.8 Hz, 1H), 4.61 (dd, *J* = 6.4 and 7.8 Hz, 1H), 3.82 (s, 3H), 3.78 (s, 3H), 3.66 (dd, *J* = 7.8 and 16.9 Hz, 1H), 3.60 (dd, *J* = 6.4 and 16.9 Hz, 1H), 2.62 (s, 3H). ¹³C NMR (75 MHz, DMSO-*d*₆) δ 171.1, 166.9, 157.4, 155.3, 150.9, 137.1, 135.5, 131.1, 129.2, 128.3, 126.3, 125.6, 117.8, 115.3, 55.8, 52.8, 51.6, 36.2, 11.5. HRMS (M + H)⁺ calcd for C₂₁H₂₀³⁵ClN₄O₃ 411.1229; found 411.1245.

Compound 7 Methyl [5-(4-Chlorophenyl)-7-(methoxy)-2-thioxo-2,3-dihydro-1H-1,4-benzodiazepin-3-yl]acetate. Yield from **6**: 81%, pale-yellow solid. ¹H NMR (300 MHz, CDCl₃) δ 10.11 (br s, 1H), 7.48 (m, 2H), 7.34 (m, 2H), 7.18 (d, *J* = 8.9 Hz, 2H), 7.11 (dd, *J* = 8.9 and 2.8 Hz, 1H), 6.78 (d, *J* = 2.8 Hz, 1H), 4.39 (dd, *J* = 7.0 and 6.8 Hz, 1H), 3.76 (s, 3H), 3.75 (s, 3H), 3.66 (dd, *J* = 16.8 and 6.8 Hz, 1H), 3.38 (dd, *J* = 16.8 and 7.0 Hz, 1H). ¹³C NMR (75 MHz, DMSO-*d*₆) δ 198.6, 171.3, 166.2, 155.4, 136.7, 135.4, 133.2, 131.1, 128.5, 128.4, 123.4, 119.0, 113.6, 63.8, 55.6, 51.3, 39.0. HRMS (M + H)⁺ calcd for C₁₉H₁₈³⁵ClN₂O₃S 389.0727; found 389.0714.

Compound 6 Methyl [5-(4-Chlorophenyl)-7-(methoxy)-2-oxo-2,3-dihydro-1H-1,4-benzodiazepin-3-yl]acetate. ¹H NMR (300 MHz, CDCl₃) δ 8.73 (br s, 1H), 7.50 (m, 2H), 7.35 (m, 2H), 7.15–7.07 (m, 2H), 6.76 (m, 1H), 4.18 (dd, *J* = 7.2 and 6.8 Hz, 1H), 3.75 (s, 3H), 3.74 (s, 3H), 3.42 (dd, *J* = 16.9 and 7.2 Hz, 1H), 3.42 (dd, *J* = 16.9 and 6.8 Hz, 1H). ¹³C NMR (75 MHz, DMSO-*d*₆) δ 171.6, 169.5, 166.6, 154.3, 137.1, 135.2, 132.7, 131.1, 128.4, 126.8, 122.9, 119.2, 113.4, 60.3, 55.5, 51.3, 35.9. HRMS (M + H)⁺ calcd for C₁₉H₁₈³⁵ClN₂O₄ 373.0955; found 373.0957.

Compound **1** was prepared as described in ref 34.

For full details of synthesis and QC, see Supporting Information, Section 1 (S2–S5).

Reagents and Plasmids (Full Details in Supporting Information, Figure 2 (S6)). Human Brd2 was cloned from human heart Marathon ready cDNA (Clontech), subcloned into pcDNA3.1D (Invitrogen) and verified by full-length DNA sequencing. Flag-Brd2 full length (1–2406 bp), Flag-Brd2 N term (1–1422 bp) and Flag-Brd2 C term (1423–2406 bp) were generated using the Gateway system (Invitrogen, San Diego, CA). Purified PCR products were subcloned into pENTR-D-TOPO and subsequently transferred into a modified pDEST16 vector containing a 5' prime FLAG tag sequence. Constructs were verified by DNA sequencing

Affinity Chromatography and Gel Electrophoresis (See Also Supporting Information, Section 4 (S16–S19)). HepG2 lysates

prepared as detailed in the Supporting Information (5 mL) were thawed on ice and cleared by centrifugation (10000g, 10 min.). The lysate was first precleared with 50 μ L of 50% slurry of blocked Reacti-gel 6× beads (with rotation, 1 h, 4 °C). The beads were pelleted by centrifugation (1000g, 1 min, 4 °C) and 1.5 mL of lysate added to a fresh tube containing 100 μ L of 50% slurry of Reacti-gel 6× beads coupled to the relevant compound and incubated with rotation for 4 h at 4 °C. For competition experiments, excess free compound or 5% DMSO control was added prior to incubation. The beads were washed 4× with 1% NP40 lysis buffer with 250 mM salt and eluted with 25 μ L of 2× SDS sample buffer (10 min, 37 °C). Samples were separated by SDS-PAGE using NuPAGE 4–12% gradient gels and then stained using GelCode Blue. For subsequent analysis by mass spectrometry, bands were excised from destained gels.

Hek293 lysates were prepared as above. From 1 mL of lysate, one-half was mixed with 25 μ L of Reacti-gel 6× beads coupled to the relevant compound and the remaining half mixed with 25 μ L Anti FLAG-M2 antibody coupled to sepharose beads. Lysates and beads were incubated with rotation for 4 h at 4 °C. The beads were washed 4× with 1% Triton X100 lysis buffer and eluted with 15 μ L of 2× SDS sample buffer (10 min, 37 °C). Samples were separated by SDS-PAGE, transferred to PVDF membrane, and immunoblotted with anti-FLAG M2 antibody.

Mass Spectrometry (Full Methods Can Be Found in Supporting Information, Section 4iv (S16–S19)). The entire lanes of the chemoproteomic gels were subjected to MS analysis and not just the visible bands as described in the Supporting Information. The manually excised gel bands were subject to automated in situ enzymatic digestion and analyzed by LC/MS/MS. Database searches were carried out using an in-house MASCOT (Matrix Science, UK)³⁰ server against the PSR protein database.

Luciferase Reporter Assay (Full Details in Supporting Information, Figure 3 (S6)). Human hepatocyte HepG2 cells (stably transfected with an ApoA1 luciferase reporter) were incubated for 18 h in the presence or absence of freshly diluted compound (0.5% DMSO) prior to addition of Bright Glo reagent (Promega). Luminescence was read using a Perkin-Elmer Envision plate reader after 10 min incubation with the substrate. The selectivity of the effect was tested using an LDL-receptor promoter luciferase reporter (HepG2LDLR Luciferase clone 2) using the same conditions in parallel.

ApoA1 Secretion Assay. Compounds were tested for their ability to increase ApoA1 production by HepG2 cells. HepG2 cells were grown in BME medium containing 10% heat inactivated FCS, glutamine, sodium pyruvate, nonessential amino acids and penicillin-streptomycin at 37 °C in a 95% air–5% CO₂ humidified atmosphere. The compounds were first incubated onto confluent HepG2 cells in BME medium containing 1% FCS and all other additives. After 48 h incubation, the supernatants were removed and compounds were read onto cells in RPMI-1640 medium depleted in methionine and cysteine and supplemented with 1% cystine, 1% glutamine, 1% penicillin–streptomycin, and ³⁵S-methionine. The incubation was maintained for 6 additional hours at 37 °C. Neosynthesized radiolabeled secreted proteins were then analyzed on 5–12% SDS Page. After exposure of gels onto Phosphor-Imager screens, radiolabeled secreted ApoA1 was quantified using a Storm 860 (Molecular Dynamics) apparatus.

Isothermal Titration Calorimetry. ITC titrations were carried out using a Microcal VP-ITC in 20 mM Hepes, pH 7.5, 100 mM NaCl at the temperatures indicated. Compound concentrations were determined by NMR and protein concentrations by A280 measurements. Typically, 10–20 μ M compound was placed in the cell and 120–240 μ M protein was titrated into this at 16–26 °C to achieve at least a final excess of 2:1 protein:ligand concentrations for single bromodomain constructs and 1.2:1 for tandem bromodomain constructs. Injections were performed using protein in the syringe rather than compound due to the limited solubility of **1**. The data was fitted within Origin (Microcal version).

Crystal Structure of BET Bromodomain Proteins with 1 and 2 (Full Details Are Available in Supporting Information, Section 7 (S34–S39)). Crystals were generated by cocrystallization and/or compound soaks into apo crystals. In some instances, structures could be generated using both methods, and as there were no significant differences in binding mode observed, structures obtained by both methods were treated equally. Crystals were generated by vapor diffusion using sitting or hanging drops. Data was collected from cryoprotected single crystals, and typically the data was processed and refined using the CCP4³¹ suite of software, with rounds of model building using Coot.³² Parts a and b–f of Figure 3 and Figure 4 were prepared using PyMOL (Schrodinger Inc.) and Figure 3b using MOE (Chemical Computing Group).

SPR Experiments (See Supporting Information, Figure 5vi (S27–S31)). Real-time monitoring of the interactions between 1 and BET bromodomains were performed on a BIAcore S51 (GE Healthcare) at 25 °C. Flow cells of a CM5 chip were first activated with 0.2 M *N*-ethyl-*N'*-(diethylaminopropyl)-carbodiimide (EDC) and 0.05 M *N*-hydroxysuccinimide (NHS). Typically 0.15 mg/mL inhibited Brd2-BD1 and Brd2-BD2 at pH 6.5 in NaAc was then injected at 10 μ L/min for 2 min, resulting in >5kRU of protein immobilized on the surface. The surface was neutralized with ethanolamine and extensively washed in the running buffer 50 mM HEPES pH7.5, 150 mM NaCl. Compounds were titrated as a tripling dilution starting at 10–20 μ M (For Figure 3e,f the concentrations were: pink = 6.7 μ M, red = 2.3 μ M, cyan = 0.74 μ M, green = 0.25 μ M, blue = 0.08 μ M, gray = 0.03 μ M, respectively). Binding curves were analyzed with BIAevaluation (GE Healthcare).

FRET Titrations. Compounds were titrated against BD12 of Brd2 (200nM), Brd3 (100nM), and Brd4 (50nM) in 50 mM HEPES pH7.5, 50 mM NaCl, 0.5 mM CHAPS in the presence of tetra-acetylated histone H4 peptide (200 nM) (Millipore, cat. 12-379). After equilibrating for 1 h, the bromodomain protein:peptide interaction was detected using FRET following the addition of 2 nM europium cryptate labeled streptavidin (Cisbio610SAKLA) and 10 nM XL-665-labeled anti-6His antibody (Cisbio 61HisXLA) in assay buffer containing 0.05% (v/v) BSA and 400 mM KF. Plates were read using an Envision Plate reader (excitation 320 nm, emission 615 and 665 nm).

RNAi (Full Details in Supporting Information, Section 4 (S7–S8,S20)). HepG2 cells were grown in Dulbecco's Modified Eagles Medium (DMEM) supplemented with 10% FCS, 1% (W/V) glutamine, and 1% pen/strep. Cells were plated at a density of 2×10^4 cells per 96-well plate, 24 h pretransfection, and siRNAs were transfected with the Gemini lipid GSK347232³³ at 7.5 μ g/mL final concentration. ApoA1 induction was measured relative to the control siRNA treated cells. Specific custom designed siRNAs targeting Brd2, Brd3, and Brd4 were used that were found to have no mRNA knockdown effect on the other family members.

Fluorescence Anisotropy (FA) Binding Assays (Full Details in Supporting Information, Section 6 (S31–S33)). Compounds were tested in dose response mode using an Alexa Fluor 488 derivative of 2 (Figure 5). Then 75 nM of Brd2, 3, or 4, 5 nM fluorescent ligand and compound were incubated for at least 1 h in 50 mM Hepes pH 7.4, 150 mM NaCl, 0.5 mM CHAPS prior to the FA being read on an Envision ($\lambda_{\text{ex}} = 485$ nm, $\lambda_{\text{em}} = 530$ nm; dichroic –505 nm).

■ ASSOCIATED CONTENT

Supporting Information. Additional figures, experimental data, material and methods. Chemical synthesis and characterization of all intermediate compounds to 1, 2, 3: biological reagents and plasmids details; luciferase reporter assay methods; chemoproteomic and siRNA: chemoproteomic and siRNA results, example gels from chemoproteomics experiments, table of proteins identified by MS on analysis of gels, chemoproteomic

material and methods, siRNA material and methods; biophysical characterization: constructs and production of single and tandem bromodomain proteins, example ITC data, KD determination of FRET H4 peptide for the tandem BET proteins, thermal shift and ITC selectivity data, matrix of sequence identify between BET bromodomains and CREBBP, ATAD2, biacore methods and analysis of cmpd1 binding to Brd-BD1/2; fluorescence anisotropy assay: correlation of FA BET binding activity with Apo-A1 upregulation, FA material and methods; X-ray crystallography: X-ray refinement statistics, Omit maps of the ligands, crystallization and crystallography material and methods, electrostatic surface of Brd2. This material is available free of charge via the Internet at <http://pubs.acs.org>.

■ Accession Codes

Atomic coordinates of Brd2-BD1:compound 1 (2ydw), Brd2-BD1:compound 2 (2yek), Brd4-BD1:compound 1 (2yel) and Brd4-BD2:compound 1 (2yem) have been deposited with the Protein Data Bank.

■ AUTHOR INFORMATION

Corresponding Author

*Phone: +44 1438 763342. Fax: +44 1438 763352. E-mail: Chun-Wa.H.Chung@gsk.com.

■ ACKNOWLEDGMENT

We thank staff at the ESRF at Genoble for beamline assistance. The Structure Genomics Consortium kindly provided cDNA for the Brd4-BD1 and Brd4-BD2 constructs. Single bromodomain construct design was performed by Pam Thomas. Mike Woodrow, Jon Seal, and Dave Wilson helped us gather together the chemical QC data. Champa Patel conducted the initial FRET assay development and members, of the Screening and Compound Profiling Department ran the BET FA assay. Finally, we acknowledge the many colleagues that have contributed to the ApoA1 program and those that have taken time to pass on useful comments in the preparation of this manuscript.

■ DEDICATION

This paper is dedicated to the memory of Dr. François Hyafil, who died on 26 May 2006.

■ ABBREVIATIONS USED

AcK, acetylated lysine; ApoA1, apolipoprotein A1; BET, bromodomain and ET domain; BD1,BD2,BD12, bromodomain 1,2,1and2; BZD, benzodiazepine; chromodomain, chromatin organization modifier domain; FA, fluorescence anisotropy; FRET, fluorescence resonance energy transfer; H4AcK₄, tetra-acetylated lysine histone 4 peptide; ITC, isothermal titration calorimetry; MOA, mode of action; PHD, plant homeodomain; SAHA, suberoylanilide hydroxamic acid; SAR, structure–activity relationships; siRNA, short interfering ribonucleic acid; SPR, surface plasmon resonance

■ REFERENCES

- (1) Goldberg, A. D.; Allis, C. D.; Bernstein, E. Epigenetics: a landscape takes shape. *Cell* **2007**, *128*, 635–638.
- (2) Kouzarides, T. Chromatin modifications and their function. *Cell* **2007**, *128*, 693–705.

- (3) Taverna, S. D.; Li, H.; Ruthenburg, A. J. How chromatin-binding modules interpret histone modifications: lessons from professional pocket pickers. *Nature Struct. Mol. Biol.* **2007**, *14*, 1025–1040.
- (4) Grant, S.; Easley, C.; Kirkpatrick, P. Vorinostat. *Nature Rev. Drug Discovery* **2007**, *6*, 21–22.
- (5) Sperandio, O.; Reynes, C. H.; Camproux, A. C.; Villoutreix, B. O. Rationalizing the chemical space of protein–protein interaction inhibitors. *Drug Discovery Today* **2009**, *15*, 220–229.
- (6) Zeng, L.; Li, J.; Muller, M.; Yan, S.; Mujtaba, S.; Pan, C.; Wang, Z.; Zhou, M.-M. Selective Small Molecules Blocking HIV-1 Tat and Coactivator PCAF Association. *J. Am. Chem. Soc.* **2005**, *127*, 2376–2377.
- (7) Sachchidanand; Resnick-Silverman, L.; Yan, S.; Mutjaba, S.; Liu, W.-j.; Zeng, L.; Manfredi, J. J.; Zhou, M.-M. Target Structure-Based Discovery of Small Molecules that Block Human p53 and CREB Binding Protein Association. *Chem. Biol.* **2006**, *13*, 81–90.
- (8) Koeller, K. M.; Haggarty, S. J.; Perkins, B. D.; Leykin, I.; Wong, J. C.; Kao, M. C.; Schreiber, S. L. Chemical genetic modifier screens: small molecule trichostatin suppressors as probes of intracellular histone and tubulin acetylation. *Chem. Biol.* **2003**, *10*, 397–410.
- (9) Johnson, R. L.; Huang, R.; Jadhav, A.; Southall, N.; Wichterman, J.; MacArthur, R.; Xia, M.; Bi, K.; Printen, J.; Austin, C. P.; Inglese, J. A quantitative high-throughput screen for modulators of IL-6 signaling: a model for interrogating biological networks using chemical libraries. *Mol. Biosyst.* **2009**, *5*, 1039–1050.
- (10) Johnson, R. L.; Huang, W.; Jadhav, A.; Austin, C. P.; Inglese, J.; Martinez, E. D. A quantitative high-throughput screen identifies potential epigenetic modulators of gene expression. *Anal. Biochem.* **2008**, *375*, 237–248.
- (11) Barter, P. J.; Nicholls, S.; Rye, K.; Anantharamaiah, G. M.; Navab, M.; Fogelman, A. M. Antiinflammatory properties of HDL. *Circ. Res.* **2004**, *95*, 764–772.
- (12) Wong, N. C. Novel therapies to increase apolipoprotein AI and HDL for the treatment of atherosclerosis. *Curr. Opin. Invest. Drugs* **2007**, *8*, 718–728.
- (13) Florence, B.; Faller, D. V. You bet-cha: a novel family of transcriptional regulators. *Front. Biosci.* **2001**, *6*, D1008–D1018.
- (14) Mirguet, O.; Ajakane, M.; Boullay, A. M.; Boursier, E.; Brusq, J.-M.; Clément, C.; Costaz, A.; Daugan, A.; Dudit, Y.; Gosmini, R.; Huët, P.; Martin, S.; Pineau, O.; Riou, A.; Toum, J.; Trotter, L.; Nicodème, E. Discovery of benzodiazepine derivatives as Apo A-1 upregulators. *Abstracts of Papers, 241st ACS National Meeting & Exposition, Anaheim, CA, United States, March 27–31, 2011*; American Chemical Society: Washington DC, 2011; MEDI-76.
- (15) Nicodème, E.; Jeffrey, K. L.; Schaefer, U.; Beinke, S.; Dewell, S.; Chung, C.; Chandwani, R.; Marazzi, I.; Wilson, P.; Coste, H.; White, J.; Kirilovsky, J.; Rice, C. M.; Lora, J. M.; Prinjha, R. K.; Lee, K.; Tarakhovskiy, A. Suppression of inflammation by a synthetic histone mimic. *Nature* **2010**, *468*, 1119–1123.
- (16) Pivrot-Pajot, C.; Caron, C.; Govin, J.; Vion, A.; Rousseaux, S.; Khochbin, S. Acetylation-dependent chromatin reorganization by BRDT, a testis-specific bromodomain-containing protein. *Mol. Cell. Biol.* **2003**, *23*, 5354–5365.
- (17) Huang, H.; Zhang, J.; Shen, W.; Wang, X.; Wu, J.; Shi, Y. Y. Solution structure of the second bromodomain of Brd2 and its specific interaction with acetylated histone tails. *BMC Struct. Biol.* **2007**, *7*, 57.
- (18) Horton, J. R.; Upadhyay, A. K.; Qi, H. K.; Zhang, X.; Shi, Y.; Cheng, X. Enzymatic and structural insights for substrate specificity of a family of jumonji histone lysine demethylases. *Nature Struct. Mol. Biol.* **2010**, *17*, 38–43.
- (19) LeRoy, G.; Rickards, B.; Flint, S. J. The double bromodomain proteins Brd2 and Brd3 couple histone acetylation to transcription. *Mol. Cell* **2008**, *30*, 51–60.
- (20) Wu, S. Y.; Chiang, C. M. The double bromodomain-containing chromatin adaptor Brd4 and transcriptional regulation. *J. Biol. Chem.* **2007**, *282*, 13141–13145.
- (21) Mujtaba, S.; Zeng, L.; Zhou, M. M. Structure and acetyl-lysine recognition of the bromodomain. *Oncogene* **2007**, *26*, 5521–5527.
- (22) Nakamura, Y.; Umehara, T.; Nakano, K.; Jang, M. K.; Shirouzu, M.; Morita, S.; Uda-Tochio, H.; Hamana, H.; Terada, T.; Adachi, N.; Matsumoto, T.; Tanaka, A.; Horikoshi, M.; Ozato, K.; Padmanabhan, B.; Yokoyama, S. Crystal structure of the human BRD2 bromodomain: insights into dimerization and recognition of acetylated histone H4. *J. Biol. Chem.* **2007**, *282*, 4193–4201.
- (23) Umehara, T.; Nakamura, Y.; Jang, M. K.; Nakano, K.; Tanaka, A.; Ozato, K.; Padmanabhan, B.; Yokoyama, S. *J. Biol. Chem.* **2010**, *285*, 7610–7618.
- (24) Vollmuth, F.; Blankenfeldt, W.; Geyer, M. Structures of the dual bromodomains of the P-TEFb-activating protein Brd4 at atomic resolution. *J. Biol. Chem.* **2009**, *284*, 36547–36556.
- (25) Moriniere, J.; Rousseaux, S.; Steuerwald, U.; Soler-Lopez, M.; Curtet, S.; Vitte, A.-L.; Govin, J.; Gaucher, J.; Sadoul, K.; Hart, D. J.; Krijgsveld, J.; Kochbin, S.; Muller, C. W.; Petosa, P. Cooperative binding of two acetylation marks on a histone tail by a single bromodomain. *Nature* **2009**, *461*, 664–668.
- (26) You, J.; Croyle, J. L.; Nishimura, A.; Ozato, K.; Howley, P. M. Interaction of the bovine papillomavirus E2 protein with Brd4 tethers the viral DNA to host mitotic chromosomes. *Cell* **2004**, *117*, 349–360.
- (27) Greenwald, R. J.; Tumang, J. R.; Sinha, A.; Currier, N.; Cardiff, R. D.; Rothstein, T. L.; Faller, D. V.; Denis, G. V. E mu-BRD2 transgenic mice develop B-cell lymphoma and leukemia. *Blood* **2004**, *103*, 1475–1484.
- (28) Filippakopoulos, P.; Qi, J.; Picaud, S.; Shen, Y.; Smith, W. B.; Fedorov, O.; Morse, E. M.; Keates, T.; Hickman, T. T.; Felletar, I.; Philpott, M.; Munro, S.; McKeown, M. R.; Wang, Y.; Christie, A. L.; West, N.; Cameron, M. J.; Schwartz, B.; Heightman, T. D.; La Thangue, N.; French, C. A.; Wiest, O.; Kung, A. L.; Knapp, S.; Bradner, J. E. Selective inhibition of BET bromodomains. *Nature* **2010**, *468*, 1067–1073.
- (29) Owen, D. J.; Ornaghi, P.; Yang, J.-C.; Lowe, N.; Evans, P. R.; Ballario, P.; Neuhaus, D.; Filetici, P.; Travers, A. A. The structural basis for the recognition of acetylated histone H4 by the bromodomain of histone acetyltransferase gcn5p. *EMBO J.* **2000**, *19*, 6141–6149.
- (30) Perkins, D. N.; Pappin, D. J.; Creasy, D. M.; Cottrell, J. S. Probability-based protein identification by searching sequence databases using mass spectrometry data. *Electrophoresis* **1999**, *20*, 3551–3567.
- (31) Collaborative Computational Project Number 4. The CCP4 suite: programs for protein crystallography. *Acta Crystallogr., Sect. D: Biol. Crystallogr.* **1993**, *50*, 760–763.
- (32) Emsley, P.; Cowtan, K. Coot: model-building tools for molecular graphics. *Acta Crystallogr., Sect. D: Biol. Crystallogr.* **2004**, *60*, 2126–2132.
- (33) Castro, M.; Griffiths, D.; Patel, A.; Patrick, N.; Kitson, C.; Ladlow, M. Effect of chain length on transfection properties of spermine-based gemini surfactants. *Org. Biomol. Chem.* **2004**, *2*, 2814–2280.
- (34) Freidinger, R. M.; Evans, B. E.; Bock, M. G. Triazolobenzodiazepines. U.S. Patent US5185331 A1, 1993.